



This is an author produced version of *Absolute and convective instabilities of parallel propagating circularly polarized Alfvén waves: Decay instability* .

White Rose Research Online URL for this paper:
<http://eprints.whiterose.ac.uk/1670/>

Article:

Ruderman, M.S. and Simpson, D. (2004) Absolute and convective instabilities of parallel propagating circularly polarized Alfvén waves: Decay instability. *Physics of Plasmas*, 11 (9). pp. 4178-4187. ISSN 1089-7674

<http://dx.doi.org/10.1063/1.1774166>

Absolute and convective instabilities of parallel propagating circularly polarized Alfvén waves: Decay instability

M. S. Ruderman^{a)} and D. Simpson

Department of Applied Mathematics, University of Sheffield, Hicks Building, Hounsfield Road, Sheffield S3 7RH, United Kingdom

(Received 9 February 2004; accepted 25 May 2004; published 29 July 2004)

The absolute and convective instabilities of circularly polarized Alfvén waves propagating along an ambient magnetic field are studied. The approximation of ideal magnetohydrodynamics is used. The analysis is restricted to the decay instability that occurs when the sound speed is smaller than the Alfvén speed. In addition, it is assumed that the amplitude a of an unstable Alfvén wave (pump wave) is small. This assumption allows us to study the problem analytically using expansions in power series with respect to a . It is shown that there are quantities, $U_l < 0$ and $U_r > 0$, such that the pump wave is absolutely unstable in a reference frame moving with velocity U with respect to the rest plasma if $U_l < U < U_r$. If either $U < U_l$ or $U > U_r$, then the pump wave is convectively unstable. The expressions for U_l and U_r are found. The signaling problem is studied in a reference frame where the pump wave is convectively unstable. It is shown that spatially amplifying waves exist only when the signaling frequency is in two narrow symmetric frequency bands with the widths of the order of a . The implication of the obtained results on the interpretation of observational data obtained in space missions is discussed. It is shown that circularly polarized Alfvén waves propagating in the solar wind are convectively unstable in a reference frame of any spacecraft moving with the velocity not exceeding a few tens of km/s in the solar reference frame. The spatial amplification scale of these waves is very large, of the order of $1/6$ a.u. In view of these results it is not surprising at all that evidence of the decay instability of Alfvén waves in the solar wind is sparse. © 2004 American Institute of Physics. [DOI: 10.1063/1.1774166]

I. INTRODUCTION

The problem of stability of finite-amplitude circularly polarized Alfvén waves has attracted the attention of plasma physicists for the last four decades. This problem has been studied both from a purely theoretical point of view and from the point of view of applications to laboratory and space plasmas. Galeev and Oraevskii¹ were the first to study this problem (see also, Sagdeev and Galeev²). This first analysis was based on the ideal magnetohydrodynamic (MHD) description and assumed that the plasma β and the Alfvén wave amplitude are small. After that the stability analysis was extended in a few different directions. Derby³ and Goldstein⁴ studied the stability of Alfvén waves with an arbitrary amplitude in a finite β plasma. Mio *et al.*,^{5,6} Mjølhus,⁷ Ovenden,⁸ and Spangler and Sheerin^{9,10} used the derivative nonlinear Schrödinger equation to study the stability of a small amplitude circularly polarized Alfvén wave in a dispersive plasma. Sakai and Sonnerup,¹¹ Longtin and Sonnerup,¹² Wong and Goldstein,¹³ and Brodin and Stenflo¹⁴ studied the stability of finite amplitude dispersive Alfvén waves on the basis of the two fluid description. Viñas and Goldstein¹⁵ studied the linear stability of circularly polarized Alfvén waves with respect to obliquely propagating perturbations. Ghosh *et al.*^{16,17} and Ghosh and Goldstein¹⁸ used numerical simulation to study nonlinear evolution of circularly polarized Alfvén waves in two dimensions. Hollweg *et al.*¹⁹ and Jayanti and Hollweg²⁰ analyzed the stability of circularly po-

larized Alfvén waves in a plasma with streaming He^{++} ions. Ling and Abraham-Srauner,²¹ Spangler,^{22,23} and Inhester²⁴ used the kinetic description to study the stability of Alfvén waves. Lou²⁵ studied the stability of circularly polarized Alfvén waves in a self-gravitating ionized medium. A comprehensive comparison of theory and observations was given by Spangler.²⁶ Among recent publications it is worth to note papers by Del Zanna *et al.*^{27,28} and by Del Zanna and Velli.²⁹ These authors developed a three-dimensional MHD code specially designed to study the stability and nonlinear evolution of Alfvén waves. They applied their numerical results to the evolution of Alfvén wave spectra in the solar wind,^{27,28} and to plasma heating in coronal holes.²⁹

The traditional treatment of the stability of circularly polarized Alfvén waves is based on the assumption that the density perturbation is proportional to $\exp[i(kx - \omega t)]$. With this ansatz for the density perturbation, the linearized MHD equations dictate how the perturbations of other quantities must vary. Jayanti and Hollweg³⁰ suggested another approach based on the use of Floquet's theorem for linear systems of differential equations with periodic coefficients. Ruderman and Simpson³¹ improved on the method developed by Jayanti and Hollweg, and carried out an analytical analysis of the general properties of the dispersion equation determining the stability of finite-amplitude circularly polarized Alfvén waves in ideal MHD. In particular, they proved that, for any wave amplitude and any plasma β , there is such an interval of wavenumbers that a harmonic perturbation is unstable if its wavenumber is in this interval and stable other-

^{a)}Electronic mail: m.s.ruderman@sheffield.ac.uk

wise. They also studied the dependence of the boundaries of the interval of unstable wavenumbers on the Alfvén wave amplitude and plasma β .

It is well known that the normal mode analysis is not sufficient to conclude whether a stationary state, homogeneous in at least one spatial direction, appears stable or unstable in a fixed reference frame. When the normal mode analysis predicts stability, the further study is not needed. However, a steady state can appear stable in a fixed reference frame even when there are growing normal modes. In this case we have to distinguish between the absolute and convective instabilities.^{32,33} The type of instability, either absolute or convective, is determined by the asymptotic behavior of the initial perturbations. Two different kinds of asymptotic behavior are possible. It is possible that the initial perturbation grows exponentially with time at any fixed spatial position. This situation is referred to as “absolute” instability. It is also possible that the initial perturbation grows exponentially with time, but simultaneously it is convected out of any finite portion of the spatial domain so fast that eventually it decays exponentially at any fixed spatial position. This situation is referred to as a “convective” instability. The concept of absolute and convective instabilities was first developed in plasma physics.^{32,33} Later it was applied to hydrodynamic stability problems, in particular, to stability of geophysical and astrophysical flows.^{34–38}

The distinction between absolute and convective instabilities is especially important for interpretation of observational results obtained during space missions. A space probe will observe an unstable circularly polarized Alfvén wave only if this wave is absolutely unstable in the reference frame of the probe. To our knowledge nobody has yet studied the absolute and convective instabilities of circularly polarized Alfvén waves. Our paper aims to fill this gap.

The paper is organized as follows. In the next section we formulate the problem and give a brief description of Briggs’ method for studying absolute and convective instabilities.³² In Sec. III we study the absolute and convective decay instabilities of small amplitude circularly polarized Alfvén waves. In Sec. IV we study the signaling problem for convectively unstable Alfvén waves. Section V contains discussion and summary.

II. FORMULATION AND METHOD DESCRIPTION

We study the stability of a circularly polarized Alfvén wave (pump wave) propagating along the mean magnetic field in the framework of ideal MHD. In Cartesian coordinates x, y, z with the x -axis in the direction of the mean magnetic field, the perturbations of the density, pressure and the x -component of the velocity in this wave remain equal to zero. The y and z -components of the velocity and the magnetic field are proportional to $\exp[i(k_0x - \omega_0t)]$, and their magnitudes are constant. The stability of this wave is determined by the following dispersion equation^{3,4,31}

$$D(\omega, k) \equiv (\omega^2 - b^2k^2)(\omega - k)[(\omega + k)^2 - 4] - a^2k^2(\omega^3 + \omega^2k - 3\omega + k) = 0. \quad (1)$$

This equation determines the stability with respect to an

eigenmode where the density perturbation is proportional to $\exp[i(Kx - \Omega t)]$. In Eq. (1), $\omega = \Omega / \omega_0$, $k = K / k_0$, and $b = c_s / v_A$, where c_s is the sound speed and v_A is the Alfvén speed calculated with the use of the ambient magnetic field B_0 . Note that $\omega_0 = v_A k_0$. The dimensionless amplitude of the Alfvén wave, a , is equal to B_\perp / B_0 , where B_\perp is the magnitude of the perpendicular component of the magnetic field in the Alfvén wave.

For any values of a and b there is such an interval (k_1, k_2) that, for any $k \in (k_1, k_2)$, Eq. (1) has exactly one root with positive imaginary part.³¹ This result implies that a circularly polarized Alfvén wave is always unstable with respect to normal modes.

As we have already mentioned, the normal mode analysis is insufficient to conclude whether or not the wave looks unstable at a fixed position. The wave does look unstable if the instability is absolute. If the instability is convective, the wave looks stable in spite of the presence of unstable eigenmodes. The type of instability, either absolute or convective, depends on the reference frame. The wave can be absolutely unstable in one reference frame and convectively unstable in another. Therefore, in what follows we study the absolute and convective instabilities in a reference frame moving with an arbitrary velocity \bar{U} along the x -axis with respect to the background plasma.

To distinguish between absolute and convective instabilities we have to solve the initial value problem for the linearized MHD equations using the Fourier transform with respect to x and the Laplace transform with respect to time. As a result, we obtain for the density perturbation the expression

$$\delta\rho(x, t) = \int_{i\tau-\infty}^{i\tau+\infty} e^{-i\omega t} d\omega \int_{-\infty}^{\infty} \frac{T(k, \omega)}{\tilde{D}(k, \omega)} e^{ikx} dk. \quad (2)$$

Here $\tilde{D}(k, \omega) = D(k, \tilde{\omega})$, where $\tilde{\omega} = \omega + kU$ is the Doppler-shifted frequency and $U = \bar{U} / v_A$ is the dimensionless velocity of the reference frame. The function $T(k, \omega)$ is determined by the initial conditions and is not important for what follows. The Bromwich integration contour $\mathcal{J}(\omega) = \tau$ (\mathcal{J} indicates the imaginary part of a quantity) is above all zeros of $\tilde{D}(k, \omega)$ considered as a function of ω , i.e., τ is larger than the maximum increment of unstable eigenmodes.

Now we give a brief description of Briggs’ method for studying absolute and convective instabilities.³² The starting point of Briggs’ method is Eq. (2). To determine if the instability is absolute or convective we have to determine the asymptotic behaviour of $\delta\rho$ as $t \rightarrow \infty$ and x is fixed. To do this we move the Bromwich integration contour down. If we manage to move it slightly below the real axis, this will mean that $\delta\rho$ decays with time exponentially and the instability is convective.

Let γ_M be the maximum increment of the instability. We will move the Bromwich integration contour down point by point. We take a point on this contour, fix its real part, ω_r , and start to decrease the imaginary part ω_i . Initially $\omega_i > \gamma_M$, which implies that the equation $\tilde{D}(k, \omega) = 0$, considered as an equation for k at fixed ω has no real roots (note that we now

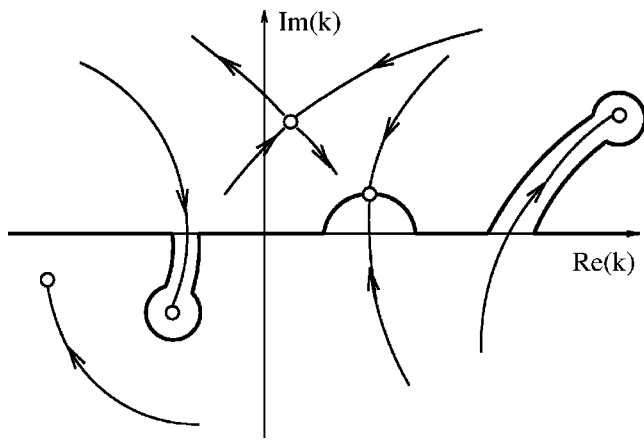


FIG. 1. The trajectories of the k -roots of the dispersion equation $\tilde{D}(k, \omega) = 0$ in the complex k -plane when $\Im(\omega)$ decreases from $\tau > \gamma_M + \epsilon$ until the pinching occurs, while $\Re(\omega)$ is fixed. The small circles indicate the end points of the trajectories and the arrows the direction of the root motion. The thick line shows the integration contour distorted to avoid singularities. We see that the two colliding roots with trajectories starting at different sides of the contour pinch the contour. The two colliding roots with trajectories starting at the same side of the contour do not pinch it.

regard k as a complex variable). Since ω_r is fixed and ω_i varies, the k -roots of the equation $\tilde{D}(k, \omega) = 0$ are functions of ω_i . When ω_i decreases, these roots move in the complex k -plane (see Fig. 1). It can occur that one of the k -roots becomes real for some value of ω_i . Then we cannot integrate along the real k -axis in Eq. (2) because the integrand has a singularity on it. However, this problem is easily cured. We simply deform the integration contour in such a way that the root trajectory does not cross the deformed contour (see Fig. 1). Since the integrand is an analytic function of k , the integral does not change.

A real problem occurs when two roots, one coming from the upper and one from the lower half of the complex k -plane, collide to form a double root as shown in Fig. 1. It is obvious that now we cannot deform the integration contour to avoid a singularity of the integrand. Hence we cannot decrease ω_i any further. The two colliding roots “pinch” the integration contour, and this is why the double root that they form is called a “pinching” root. Of course, it is also possible that two roots both coming either from the upper or from the lower part of the complex k -plane collide to form a double root. It is clearly seen in Fig. 1 that these roots do not pinch the integration contour, and this is why the double root that they form is called a “nonpinching” root.

It is clear from the previous analysis that the Bromwich integration contour can be moved below the real ω -axis if the pinching does not occur for any fixed ω_r and any $\omega_i \geq 0$. In this case $\delta\rho$ given by Eq. (2) decays exponentially as $t \rightarrow \infty$ and the instability is convective. On the other hand, if pinching occurs for some ω_r and $\omega_i > 0$, then we cannot move the Bromwich integration contour below the real axis in the complex ω -plane.

In what follows we assume that there are only a finite number of pinching roots, say, n . Let pinching occur when $\omega_r = \omega_{rj}$ and $\omega_i = \omega_{ij}$, $j = 1, \dots, n$. Then the asymptotic behavior of $\delta\rho$ as $t \rightarrow \infty$ is given by³²

$$\delta\rho \propto t^{-1/2} \exp[t(\omega_{im} - i\omega_{rm})], \tag{3}$$

where $\omega_{im} = \max_j(\omega_{ij})$.

The analysis in this section implies the following method of studying the absolute and convective instabilities.

- (i) First we have to calculate the maximum growth rate of the instability γ_M .
- (ii) Then we have to calculate all double-roots of the dispersion equation. These roots satisfy the two equations

$$\tilde{D}(k, \omega) = 0, \quad \frac{\partial \tilde{D}}{\partial k} = 0. \tag{4}$$

This system of equations determines double roots, k , and corresponding values of ω .

- (iii) Now we consider all pairs of solutions to Eq. (4), (k, ω) , and choose only those with ω satisfying the inequality

$$0 < \omega_i \leq \gamma_M. \tag{5}$$

We consider only pairs with $\omega_i > 0$ because pairs with $\omega_i \leq 0$ cannot cause absolute instability. The reason why we reject pairs with $\omega_i > \gamma_M$ is the following. Let $(\bar{k}, \bar{\omega})$ be a solution of Eq. (4) and $\bar{\omega}_i > \gamma_M$. We always can take $\tau < \bar{\omega}_i$ in Eq. (2). Then the double root \bar{k} cannot appear as a result of a collision of two k -roots when the Bromwich integration contour is moved down. If there are no pairs (k, ω) with ω_i satisfying Eq. (5) then the instability is convective.

- (iv) Among all pairs (k, ω) satisfying Eq. (5) we retain only those where k is a pinching double root. To verify that k is pinching, we fix ω_r and increase the imaginary part of ω from ω_i to $\gamma_M + \epsilon$, where ϵ is any positive quantity. As a result we obtain the trajectories of the two k -roots that collide at the point k of the complex k -plane. If the end-points of these trajectories are on different sides of the real axis in the complex k -plane, then the double root is pinching. Otherwise it is nonpinching.
- (v) Finally, among all pairs (k, ω) satisfying Eq. (5) and the condition that k is pinching, we choose one with the largest ω_i (of course it is possible that there are a few pairs with the same ω_i). Using the notation ω_{im} for this largest value of ω_i , we obtain that the asymptotic behavior of the density perturbation is given by Eq. (3).

III. ABSOLUTE AND CONVECTIVE DECAY INSTABILITIES OF SMALL-AMPLITUDE ALFVÉN WAVES

Using Eq. (1) we write the system of Eqs. (4) determining the double k -roots in the form

$$(\tilde{\omega}^2 - b^2 k^2)(\tilde{\omega} - k)[(\tilde{\omega} + k)^2 - 4] - a^2 k^2(\tilde{\omega}^3 + \tilde{\omega}^2 k - 3\tilde{\omega} + k) = 0, \tag{6}$$

$$\begin{aligned} &\bar{\omega}^4 - 2(1 + b^2)\bar{\omega}^3k - 3(1 + b^2)\bar{\omega}^2k^2 + 4b^2\bar{\omega}k^3 + 5b^2k^4 \\ &+ 4\bar{\omega}^2 + 8b^2\bar{\omega}k - 12b^2k^2 - a^2k(2\bar{\omega}^3 + 3\bar{\omega}^2k - 6\bar{\omega} \\ &+ 3k) + U[5\bar{\omega}^4 + 4\bar{\omega}^3k - 3(1 + b^2)\bar{\omega}^2k^2 \\ &- 2(1 + b^2)\bar{\omega}k^3 + b^2k^4 - 12\bar{\omega}^2 + 8\bar{\omega}k + 4b^2k^2 \\ &- a^2k^2(3\bar{\omega}^2 + 2k\bar{\omega} - 3)] = 0. \end{aligned} \tag{7}$$

Let us introduce the phase velocity in the moving reference frame $c = \bar{\omega}/k$. Then we can reduce the system of equations Eqs. (6) and (7) to

$$k^2 = \frac{4(c - 1)(c^2 - b^2) - a^2(3c - 1)}{(c + 1)[c^4 - (1 + a^2 + b^2)c^2 + b^2]}, \tag{8}$$

$$\begin{aligned} &4(1 + U)(c + 1)(c - 1)^2(c^2 - b^2)^2 - a^2\{[c^6 + 4c^5 - 3c^4 \\ &- 2(1 + 3b^2)c^3 + 3b^2c^2 + 4b^2c - b^2] + U[6c^5 - 2c^4 \\ &- (5 + 7b^2)c^3 + 4b^2c^2 + (1 + 5b^2)c - 2b^2]\} \\ &+ a^4[2c^3 + U(3c^3 - c)] = 0. \end{aligned} \tag{9}$$

Jayanti and Hollweg³⁹ have used the Alfvén wave amplitude a as a small parameter. As a result they have managed to study the dispersion equation (1) analytically. In particular, they have calculated the maximum increment of the instability.

In this paper we follow the approach adopted by Jayanti and Hollweg and also consider a as a small parameter. In what follows we study only the decay ($b < 1$) instability. The beat instability ($b > 1$) will be studied in the accompanying paper. Hence, in what follows, we take $0 < b < 1$. In addition we assume that b is not close to 0 or to 1.

A. Calculation of the double roots

The maximum increment of the decay instability with the accuracy up to the first nonzero term in the expansion with respect to a is given by³⁹

$$\gamma_M = \frac{a(1 - b)^{1/2}}{2b^{1/2}(1 + b)}. \tag{10}$$

Now we calculate the double roots of the dispersion equation considered as an equation for k . We start from calculating the roots of Eq. (9). When $a = 0$, Eq. (9) has seven roots: $c_1 = -1$, $c_{2,3} = 1$, $c_{4,5} = b$, and $c_{6,7} = -b$. In the next order approximation with respect to a we obtain

$$c_1 = -1 - \frac{a^2}{4(1 - b^2)} + \mathcal{O}(a^3), \tag{11}$$

$$c_{2,3} = 1 + \frac{a^2}{2(1 - b^2)} \pm \frac{a^3}{8} \left[\frac{2(1 - U)}{(1 + U)(1 - b^2)^3} \right]^{1/2} + \mathcal{O}(a^4), \tag{12}$$

$$c_{4,5} = b \pm \frac{a}{4} \left[\frac{(1 - b)(U - b)}{b(1 + U)} \right]^{1/2} + \mathcal{O}(a^2), \tag{13}$$

$$c_{6,7} = -b \pm \frac{a}{4} \left[\frac{-(1 + b)(U + b)}{b(1 + U)} \right]^{1/2} + \mathcal{O}(a^2). \tag{14}$$

In Eqs. (12)–(14) the upper signs correspond to c_2 , c_4 , and c_6 , and the lower signs to c_3 , c_5 , and c_7 , respectively. We use the agreement that the square root of a positive quantity is positive, and the square root of a negative quantity is purely imaginary with a positive imaginary part. Although only the first two terms are given in the expansion for c_1 , it is easy to show that all terms in this expansion are real. The expansions Eqs. (12)–(14) are valid only if $|1 + U| \gg a^2$. The case where $|1 + U| = \mathcal{O}(a^2)$ will be discussed later.

Now we use Eqs. (8) and (11)–(14) to obtain seven pairs of double k -roots:

$$k_{1\pm} = \pm \frac{8i(1 - b^2)}{a^2} + \mathcal{O}(1), \tag{15}$$

$$k_{2,3\pm} = \pm \left\{ 1 - \frac{a^2}{4(1 - b^2)} \mp \frac{a^3U}{4(1 - b^2)^{3/2}[2(1 - U^2)]^{1/2}} \right\} + \mathcal{O}(a^4), \tag{16}$$

$$k_{4,5\pm} = \pm \left\{ \frac{2}{1 + b} \mp \frac{a(1 - b)^{1/2}(1 - b + 2U)}{2(1 + b)^2[b(U + 1)(U - b)]^{1/2}} \right\} + \mathcal{O}(a^2), \tag{17}$$

$$k_{6,7\pm} = \pm \left\{ \frac{-2}{1 - b} \pm \frac{a(1 + b)^{1/2}(1 + b + 2U)}{2(1 - b)^2[-b(U + 1)(U + b)]^{1/2}} \right\} + \mathcal{O}(a^2). \tag{18}$$

In Eq. (16) the upper sign at the last term in the curly brackets corresponds to k_2 , and the lower sign to k_3 . The “+” and “-” signs at the curly brackets correspond to $k_{2,3+}$ and $k_{2,3-}$, respectively. The same rules are applicable to Eqs. (17) and (18).

B. Selection of double roots corresponding to positive increments not exceeding the maximum increment

Using the relation $\omega = k(c - U)$, we obtain the values of ω corresponding to the double k -roots:

$$\omega_{1\pm} = \pm \frac{8i(1 - b^2)(1 + U)}{a^2} + \mathcal{O}(1), \tag{19}$$

$$\omega_{2,3\pm} = \pm \left\{ 1 - U + \frac{a^2(1 + U)}{4(1 - b^2)} \pm \frac{a^3}{8} \left[\frac{2(1 - U^2)}{(1 - b^2)^3} \right]^{1/2} \right\} + \mathcal{O}(a^4), \tag{20}$$

$$\omega_{4,5\pm} = \pm \left\{ \frac{2(b - U)}{1 + b} \pm \frac{a[(1 - b)(U + 1)(U - b)]^{1/2}}{b^{1/2}(1 + b)^2} \right\} + \mathcal{O}(a^2), \tag{21}$$

$$\omega_{6,7\pm} = \pm \left\{ \frac{2(b+U)}{1-b} \pm \frac{a[-(1+b)(U+1)(U+b)]^{1/2}}{b^{1/2}(1-b)^2} \right\} + \mathcal{O}(a^2). \tag{22}$$

Now we proceed to the third step of the analysis as described in Sec. II and retain only the double-roots corresponding to ω with the imaginary part between 0 and γ_M . First of all, it is obvious that $\Im(\omega_{1\pm})$ is either negative or larger than γ_M . Hence, we reject $k_{1\pm}$.

$\Im(\omega_{2,3\pm}) \neq 0$ only if $|U| > 1$. In this case $0 < \Im(\omega_{2+}) = \Im(\omega_{3-}) < \gamma_M$, and $\Im(\omega_{2-}) = \Im(\omega_{3+}) < 0$. Hence, we retain k_{2+} and k_{3-} , and reject k_{2-} and k_{3+} .

$\Im(\omega_{4,5\pm}) \neq 0$ only if $-1 < U < b$. In this case $\Im(\omega_{4-}) = \Im(\omega_{5+}) < 0$, so we reject k_{4-} and k_{5+} . On the other hand, $\Im(\omega_{4+}) = \Im(\omega_{5-}) > 0$, and it is straightforward to show that $\Im(\omega_{4+}) < \gamma_M$. Therefore, we retain k_{4+} and k_{5-} .

$\Im(\omega_{6,7\pm}) \neq 0$ only if either $U < -1$ or $U > -b$. In that case $\Im(\omega_{6-}) = \Im(\omega_{7+}) < 0$, so that we reject k_{6-} and k_{7+} . On the other hand, $\Im(\omega_{6+}) = \Im(\omega_{7-}) > 0$. The condition $\Im(\omega_{6+}) < \gamma_M$ reduces to $U_- < U < U_+$, where

$$U_{\pm} = -\frac{b+1}{2} \pm \frac{(1-b)(1+3b^2)^{1/2}}{2^{1/2}(1+b)^{3/2}}. \tag{23}$$

It is straightforward to show that $U_- < -1 < -b < U_+$. Summarizing, we conclude that the inequality $0 < \Im(\omega_{6+}) < \gamma_M$ is satisfied if and only if U satisfies the condition

$$U_- < U < -1 \text{ or } -b < U < U_+. \tag{24}$$

Hence we retain k_{6+} and k_{7-} only if Eq. (24) is satisfied and reject otherwise.

C. Selection of pinching double roots

In the last step of the analysis we have to ascertain whether or not the retained double-roots are pinching. We start this last step of the analysis with one note. It is easy to see that $k_{3-} = -k_{2+}^*$, $k_{5-} = -k_{4+}^*$, and $k_{7-} = -k_{6+}^*$, where the asterisk indicates a complex conjugate quantity. The same relations are valid for the frequencies: $\omega_{3-} = -\omega_{2+}^*$, $\omega_{5-} = -\omega_{4+}^*$, and $\omega_{7-} = -\omega_{6+}^*$. Obviously, if the pair (k, ω) satisfies Eq. (6), then the pair $(-k^*, -\omega^*)$ also satisfies Eq. (6). This implies that the trajectories of the roots that collide to form the double root k_{2+} , and the trajectories of the roots that collide to create the double root k_{3-} , are symmetric to each other with respect to the imaginary axis in the complex k -plane. Hence, the roots k_{2+} and k_{3-} are either both pinching or both nonpinching. The same is true for k_{4+} and k_{5-} , and for k_{6+} and k_{7-} . This observation enables us to restrict the analysis to the roots k_{2+} , k_{4+} , and k_{6+} .

Let us now study the behavior of the trajectories of the roots that collide at $k = k_{2+}$. To do this we take $\omega = \omega_{2+} + ia\sigma$, where σ varies from 0 to $\sigma_2 + \epsilon$ with $\sigma_2 = [\gamma_M - \Im(\omega_{2+})]/a$ and $\epsilon > 0$. Then we substitute $\omega = 1 - U + a\bar{\omega}$ in Eq. (6) and look for the solution to the obtained equation in the form $k = 1 + a\bar{k}$. As a result we obtain

$$\begin{aligned} \bar{\omega}^2 + 2U\bar{\omega}\bar{k} + \bar{k}^2(U^2 - 1) \\ = a \frac{\bar{\omega} + \bar{k}(U+1)}{2(1-b^2)} \\ + \frac{a^2}{4(1-b^2)} \left[\frac{(7+b^2)\bar{k}^2}{2(1-b^2)} + \bar{k}(\bar{\omega} + \bar{k}U) \right. \\ \left. - \frac{(1+7b^2)(\bar{\omega} + \bar{k}U)^2}{2(1-b^2)} \right] + \mathcal{O}(\chi a^3), \end{aligned} \tag{25}$$

where $\chi = 1$ when $\sigma \sim 1$ and $\chi = a^2$ when $\sigma \leq a$. Equation (25) is a quadratic equation with respect to \bar{k} and its solution is straightforward. Taking into account the relation $k = 1 + a\bar{k}$ and Eq. (16) determining k_{2+} , the two roots of Eq. (6) close to unity are given by

$$\begin{aligned} k^{\pm} = k_{2+} + \frac{ia}{U^2 - 1} \left\{ -U\sigma \pm \left[\sigma^2 + \frac{a^2\sigma(1+b^2)}{(1-b^2)^2} \right. \right. \\ \left. \left. + \frac{a^2\sigma(U^2 - 1)^{1/2}}{[2(1-b^2)]^{3/2}} \right]^{1/2} \right\} + \mathcal{O}(\chi^{1/2}a^3). \end{aligned} \tag{26}$$

When $\sigma = 0$, $k^+ = k^- = k_{2+}$ as it should be. Let U be positive (recall that we consider $U^2 > 1$). Then $\Im(k_{2+}) > 0$ and $\Im(k^-)$ decreases monotonically when σ increases from 0 to $\sigma_2 + \epsilon$. $\Im(k^+)$ increases when σ varies from 0 to σ_M given by

$$\sigma_M = \frac{a^2\{4(1+b^2) + [2(1-b^2)(U^2 - 1)]^{1/2}\}}{16(1-b^2)^2\{[U(U-1)]^{1/2} + U - 1\}} < \sigma_2. \tag{27}$$

Then $\Im(k^+)$ decreases monotonically when σ varies from σ_M to $\sigma_2 + \epsilon$. $\Im(k^{\pm}) = -a\sigma_2/(U \pm 1) < 0$ at $\sigma = \sigma_2$. Since both $\Im(k^+)$ and $\Im(k^-)$ are monotonically decreasing functions for $\sigma > \sigma_M$, we conclude that $\Im(k^{\pm}) < 0$ at $\sigma = \sigma_2 + \epsilon$. We see that both roots, k^+ and k^- , come from the same side of the real axis. This implies that k_{2+} is not a pinching double root.

When $U < 0$, $\Im(k_{2+}) < 0$ and $\Im(k^+)$ increases monotonically when σ varies from 0 to $\sigma_2 + \epsilon$. $\Im(k^-)$ decreases when σ varies from 0 to σ_M . Then $\Im(k^-)$ increases when σ varies from σ_M to $\sigma_2 + \epsilon$. $\Im(k^{\pm}) = -a\sigma_2/(U \pm 1) > 0$ at $\sigma = \sigma_2$. Since $\Im(k^+)$ and $\Im(k^-)$ are monotonically increasing functions for $\sigma > \sigma_M$, we conclude that $\Im(k^{\pm}) > 0$ at $\sigma = \sigma_2 + \epsilon$. Once again this implies that k_{2+} is not a pinching double root. Summarizing, we conclude that k_{2+} is not a pinching double root for $U > 1$ or $U < -1$.

Note that the trajectories of the two colliding roots are on the line $\Re(k) = \Re(k_{2+})$ (\Re indicates the real part of a quantity), so that the trajectories partly overlap. This peculiar behavior of the trajectories is attributed to the approximation that we use. If we continue the calculation to the next order approximation, then we would obtain that the real parts of k^+ and k^- are different when $\sigma \neq 0$, and the trajectories would not overlap anymore. We do not carry out this calculation because it would not affect our main conclusion that the double root k_{2+} is not pinching.

Now we proceed to the trajectories of the roots that collide at $k = k_{4+}$. We take $\omega = \omega_{4+} + ia\sigma$, where σ varies from 0 to $\sigma_4 + \epsilon$ with $\sigma_4 = [\gamma_M - \Im(\omega_{4+})]/a$ and $\epsilon > 0$. We assume that $-1 < U < b$, so that $\Im(\omega_{4+}) > 0$. We look for the solution to

Eq. (6) in the form $k=2/(1+b)+\bar{k}a$. Substituting this expression into Eq. (6), we arrive at the quadratic equation for \bar{k}

$$(U+1)(b-U)\bar{k}^2 - (2U+1-b)\bar{\omega}\bar{k} - \bar{\omega}^2 - \frac{1-b}{4b(1+b)^2} = \mathcal{O}(a), \tag{28}$$

where

$$\bar{\omega} = i\sigma + \frac{i[(1-b)(U+1)(b-U)]^{1/2}}{b^{1/2}(1+b)^2}. \tag{29}$$

The solution of Eq. (28) is straightforward and eventually we obtain for the roots colliding at k_{4+} the expressions

$$k^\pm = k_{4+} + \frac{ia}{2(U+1)(b-U)} \{ (2U+1-b)\sigma \pm [(1+b)^2\sigma^2 + 2\sigma b^{-1/2}((1-b)(U+1)(b-U))^{1/2}]^{1/2} \} + \mathcal{O}(a^2). \tag{30}$$

When $2U+1-b > 0$, $\Im(k^+)$ is a monotonically increasing function of σ . Since $\Im(k_{4+}) > 0$, it follows that $\Im(k^+) > 0$ for any $\sigma > 0$ and the trajectory of k^+ does not cross the real axis. It is easy to show that $\Im(k^-)$ is a monotonically decreasing function of σ , and $\Im(k^-) = \mathcal{O}(a^2)$ at $\sigma = \sigma_4$. Then it follows that $\Im(k^-) < 0$ at $\sigma = \sigma_4 + \epsilon$ when ϵ is not too small, so that the trajectory of k^- crosses the real axis once. Hence we conclude that k_{4+} is a pinching double root.

When $2U+1-b < 0$, it follows that $\Im(k_{4+}) < 0$, and once again $\Im(k^+)$ is a monotonically increasing function of σ , and $\Im(k^-)$ is a monotonically decreasing function of σ . In addition, $\Im(k^+) = \mathcal{O}(a^2)$ at $\sigma = \sigma_4$, so that $\Im(k^+) > 0$ at $\sigma = \sigma_4 + \epsilon$ when ϵ is not too small. Hence, the trajectory of k^- does not cross the real axis, while the trajectory of k^+ crosses the real axis once. This implies that, once again, k_{4+} is a pinching double root.

Finally, we consider the trajectories of the two roots that collide at k_{6+} . We take $\omega = \omega_{6+} + ia\sigma$ with σ varying from 0 to $\sigma_6 + \epsilon$, where $\sigma_6 = [\gamma_M - \Im(\omega_{6+})]/a$, and $\epsilon > 0$. Now we look for the solutions to Eq. (6) in the form $k = -2/(1-b) + a\bar{k}$. Substituting this expression in Eq. (6) we obtain the quadratic equation for \bar{k} ,

$$(U+1)(U+b)\bar{k}^2 + (2U+1+b)\bar{\omega}\bar{k} + \bar{\omega}^2 - \frac{1+b}{4b(1-b)^2} = \mathcal{O}(a), \tag{31}$$

where

$$\bar{\omega} = i \left\{ \sigma + \frac{(1+b)^{1/2}[(U+1)(U+b)]^{1/2}}{b^{1/2}(1-b)^2} \right\}. \tag{32}$$

The solution of Eq. (31) is straightforward, and eventually we arrive at the following expression for the two roots colliding at k_{6+} :

$$k^\pm = k_{6+} + \frac{ia\sigma^{1/2}}{2(U+1)(U+b)} \{ -(2U+1+b)\sigma^{1/2} \pm [(1-b)^2\sigma + 2b^{-1/2}((1+b)(U+1)(U+b))^{1/2}]^{1/2} \} + \mathcal{O}(a^2). \tag{33}$$

We see that $k^+ = k^- = k_{6+}$ when $\sigma = 0$. For $2U+1+b > 0$ we obtain $\Im(k_{6+}) < 0$ and $\Im(k^-)$ is a monotonically decreasing function of σ , so that the trajectory of k^- does not cross the real axis. Lengthy but straightforward calculation results in the relation

$$\Im(k^-)\Im(k^+) = \frac{a^2(1+3b^2)(U+1)(U+b)}{2b(1-b^2)^2} > 0, \tag{34}$$

valid when $\sigma = \sigma_6$. Since $\Im(k^-) < 0$, we conclude that $\Im(k^+) < 0$. Then, taking ϵ small enough, we can guarantee that $\Im(k^+) < 0$ at $\sigma = \sigma_6 + \epsilon$. Depending on b and U , $\Im(k^+)$ can either be a monotonic or nonmonotonic function of σ . In the latter case the trajectory of k^+ can cross the real axis, however, it always returns to the lower part of the complex k -plane when σ increases up to $\sigma_6 + \epsilon$. Hence, the trajectory of k^+ either crosses the real axis an even number of times, or does not cross it at all. This analysis leads to the conclusion that k_{6+} is not a pinching double root.

In the case when $2U+b+1 < 0$ the analysis is quite similar. Now $\Im(k_{6+}) > 0$ and $\Im(k^+)$ is a monotonically increasing function of σ , so that the trajectory of k^+ does not cross the real axis. It follows from Eq. (34) that $\Im(k^-) > 0$ at $\sigma = \sigma_6$. Once again, taking ϵ small enough, we can guarantee that $\Im(k^-) > 0$ at $\sigma = \sigma_6 + \epsilon$, so that the trajectory of k^- either crosses the real axis an even number of times, or does not cross it at all. Hence, we conclude that k_{6+} is not a pinching double root. Note that, similar to the trajectories of the roots colliding at k_{2+} , the trajectories of the roots colliding at k_{6+} partly overlap. The discussion of this phenomenon given in the case of the double root k_{2+} is also applicable to the case of the double root k_{6+} .

D. Summary

Summarizing the analysis of this section, we conclude that, in the case when $-1 < U < b$, there are two pinching double roots, k_{4+} and k_{5-} , corresponding to the same increment

$$\gamma = \Im(\omega_{4+}) = \Im(\omega_{5-}) = \frac{a[(1-b)(U+1)(b-U)]^{1/2}}{b^{1/2}(1+b)^2} + \mathcal{O}(a^2). \tag{35}$$

When $U < -1$ or $U > b$, there are no pinching double roots corresponding to ω with a positive imaginary part. Hence, the circularly polarized Alfvén wave is absolutely unstable if $-1 < U < b$, and convectively unstable otherwise. We obtain the maximum increment, $\gamma = \gamma_M$, when $U = (b-1)/2$, which is equal to the group velocity of the wave mode that has the maximum growth rate.³⁹ This result is in complete agreement with the general theory of absolute and convective instabilities.^{32,33}

Let us make a comment on the accuracy of the expressions for the lower and upper boundaries of the absolute instability. We observe that the second term in Eq. (21) is of the order of neglected terms, $\mathcal{O}(a^2)$, when $U-b=\mathcal{O}(a^2)$. Hence, in this case we cannot claim that $\Im(\omega_{4+})>0$ even when $U>b$. Therefore, the upper boundary of the absolute instability is $U_r=b+\mathcal{O}(a^2)$.

When $U=-1+\bar{U}a$, where $\bar{U}\neq 0$ and $|\bar{U}|$ is of the order of unity, the analysis has to be modified. The term $\mathcal{O}(a^4)$ on the right-hand side of Eq. (12) has to be substituted by $\mathcal{O}(a^{7/2})$, and the terms $\mathcal{O}(a^2)$ on the right-hand sides of Eqs. (13) and (14) by $\mathcal{O}(a^{3/2})$. As a result, the last term on the right hand side of Eq. (21) will be $\mathcal{O}(a^{3/2})$ instead of $\mathcal{O}(a^2)$. This implies that the neglected terms in Eq. (21) are of the same order as the second term in the curly brackets and we cannot guarantee that $\Im(\omega_{4+})$ is positive when $U=-1+\bar{U}a$ with $\bar{U}>0$. This means that the lower boundary of the absolute instability is $U_l=-1+\mathcal{O}(a)$.

We can give a simple physical interpretation of the result that the instability is absolute in a reference frame moving with the velocity U satisfying $-1<U<b$. The decay instability is a decay of the pump wave in the forward propagating sound wave and backward propagating Alfvén wave (i.e., Jayanti and Hollweg³⁹). As a result of the instability, the both waves grow at expense of the pump wave. Let $\omega=\omega_{fs}(k)$ be the dispersion relation for the forward propagating sound wave, and $\omega=\omega_{bA}(k)$ be the dispersion relation for the backward propagating Alfvén wave. Then, for small a , $\Re(\omega_{fs})\approx bk$, $\Re(\omega_{bA})\approx 2-k$, while $\Im(\omega_{fs})\sim\Im(\omega_{bA})\sim a$. In general, the concept of group velocity is irrelevant for growing perturbations. However, we still can use this concept for *slowly* growing waves, i.e., for waves with the increment much smaller than the frequency. For such waves we determine the group velocity as $d\Re(\omega)/dk$. In the case of stable waves the energy propagates with the group velocity. For slowly growing waves it propagates *approximately* with the group velocity.

The group velocities of the forward propagating sound wave and the backward propagating Alfvén wave are $d\Re(\omega_{fs})/dk\approx b$ and $d\Re(\omega_{bA})/dk\approx -1$, respectively. This means that the energy propagates approximately with speed b in the forward direction and with speed 1 in the backward direction. Then, for large t , the perturbed portion of the spatial domain is determined by the approximate inequality $-t<x<bt$ in the plasma rest reference frame. If x' is the spatial coordinate in a reference frame moving with velocity U with respect to the plasma rest reference frame, then $x'=x-Ut$. It follows that the perturbed portion of the spatial domain in this new reference frame is determined by the approximate inequality $-t(1+U)<x'<(b-U)t$. The instability is absolute if the left boundary of this interval is moving backward, and the right boundary is moving forward. This condition results in $-1<U<b$. When $U<-1$, the left boundary is moving forward, the perturbed portion of the spatial domain is swept away, and the instability is convective. When $U>b$, the right boundary is moving backward. Once again the perturbed portion of the spatial domain is swept away, and the instability is convective.

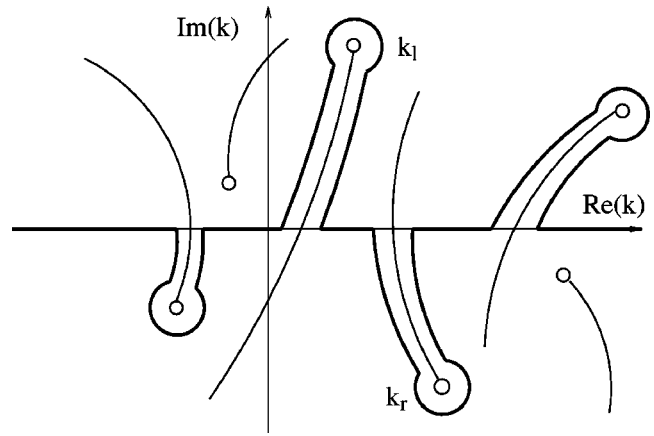


FIG. 2. The trajectories of the k -roots of the dispersion equation $\tilde{D}(k, \omega) = 0$ in the complex k -plane when $\Im(\omega)$ decreases from $\tau > \gamma_M + \epsilon$ to 0 while $\Re(\omega) = \omega_d$. The small circles indicate the end points of the trajectories. The thick line shows the integration contour distorted to avoid singularities.

IV. SPATIALLY AMPLIFYING WAVES

A. Theory

When the pump wave is convectively unstable but absolutely stable, spatially amplifying perturbations can be excited by a localized source of perturbations periodic in time.³² A problem of asymptotic response of the system to such perturbations when $t \rightarrow \infty$, is called a signaling problem. From the physical point of view, it is very important to determine the frequencies of the localized perturbations for which the asymptotic response is amplifying in space. Signaling with such frequencies can trigger nonlinear effects that may either lead to the transition to a different laminar base state, or cause the transition to turbulence. Since the pump wave is absolutely stable, an initial perturbation causes the emergence of an unstable propagating wave packet which, for $t \rightarrow \infty$, decays in every spatially bounded region, thus making no effect on the spatial structure formation through signaling.

The signaling problem can be, therefore, formulated as the initial value problem in which the initial conditions are taken to be zero and there is an external perturbation of the form $f(x, t) = f_0(x)H(t)e^{-i\omega_d t}$, where $f_0(x)$ is a function with a finite support, i.e., it is identically zero outside a finite interval, ω_d is real, and $H(t)$ is the Heaviside step function ($H(t)=0$ for $t<0$, $H(t)=1$ for $t>0$). Then in the convectively unstable case, instead of Eq. (2) we obtain

$$\delta\rho(x, t) = \int_{i\tau-\infty}^{i\tau+\infty} \frac{e^{-i\omega_d t}}{\omega - \omega_d} d\omega \int_{-\infty}^{\infty} \frac{S(k, \omega)}{\tilde{D}(k, \omega)} e^{ikx} dk, \tag{36}$$

where the function $S(k, \omega)$ depends on the external perturbation. Note that $S(k, \omega)$ is an analytic function of k and ω .

As in the previous section, we consider the trajectories of all k -roots of $\tilde{D}(k, \omega) = 0$ in the complex k -plane (see Fig. 2). Since the instability is convective, there are no pinching roots corresponding to ω with positive imaginary part. If we assume that either U is slightly smaller than U_l or slightly larger than U_r , then there are also no pinching roots corresponding to ω with $\Im(\omega) = 0$. This implies that we can shift

the Bromwich integration contour in the ω -plane slightly below the real axis everywhere except a small vicinity of $\omega = \omega_d$. Then it immediately follows that the asymptotic behavior as $t \rightarrow \infty$ is given by $\delta\rho = F(x)e^{-i\omega_d t}$, where

$$F(x) = W \int_C \frac{S(k, \omega)}{\tilde{D}(k, \omega)} e^{ikx} dk, \tag{37}$$

W is a nonzero constant, and C is the integration contour in the complex k -plane distorted to avoid singularities of the integrand when $\Im(\omega)$ decreases from $\tau > \gamma_M$ to 0 while $\Re(\omega) = \omega_d$.

Let us first study the asymptotic behavior of $F(x)$ as $x \rightarrow \infty$. It is straightforward to see that these asymptotic behavior is determined by the root with the trajectory starting in the upper part of the complex k -plane that has the smallest imaginary part at the end of its trajectory. If we denote this root as k_r , then $F(x) \sim e^{ik_r x}$ as $x \rightarrow \infty$. The rate of spatial amplification is $\gamma_r^s = -\Im(k_r)$. If all roots with trajectories starting in the upper complex k -plane have positive imaginary parts at the end of their trajectories, then there are no spatially amplifying waves propagating to the right.

The same analysis is applicable to the case where $x \rightarrow -\infty$. The only difference is that now the asymptotic behavior of $F(x)$ is determined by the root with the trajectory starting in the lower part of the complex k -plane that has the largest imaginary part at the end of its trajectory. If we denote this root as k_l , then $F(x) \sim e^{ik_l x}$ as $x \rightarrow -\infty$. The rate of spatial amplification is $\gamma_l^s = \Im(k_l)$. If all roots with trajectories starting in the lower complex k -plane have negative imaginary parts, then there are no spatially amplifying waves propagating to the left.

B. Calculations

In accordance with the analysis of the last subsection, in order to study the signaling problem we have to find the trajectories of the k -roots of (6) when $\Re(\omega) = \omega_d$ and $a\sigma = \Im(\omega)$ decreases from $\gamma_M + a\epsilon$ to 0, where $\epsilon > 0$. When doing so we assume that the instability is convective, i.e., either $U < U_l = -1 + \mathcal{O}(a)$, or $U > U_r = b + \mathcal{O}(a^2)$. We look for the solutions to Eq. (6) in the form of power series with respect to a . When ω is real ($\sigma = 0$) and $a = 0$, Eq. (6) has five real roots. It is straightforward to see that the roots of Eq. (6) remain real in any order approximation with respect to a if the difference between any two roots in the zeroth-order approximation is of the order of unity. This means that in this case there are no spatially amplifying waves. Complex roots of Eq. (6) can appear only when there are at least two roots such that the difference between them is of order a or smaller. This can occur only when $\omega_d = \bar{\omega}_{dj} + a\lambda$, where λ is real and $\bar{\omega}_{dj}$ ($j = 1, \dots, 6$) are given by

$$\begin{aligned} \bar{\omega}_{d1,2} &= \pm(1 - U), & \bar{\omega}_{d3,4} &= \pm \frac{2(b - U)}{1 + b}, \\ \bar{\omega}_{d5,6} &= \pm \frac{2(U + b)}{1 - b}. \end{aligned} \tag{38}$$

Note that $\bar{\omega}_{d1,2}$, $\bar{\omega}_{d3,4}$ and $\bar{\omega}_{d5,6}$ coincide with the first terms of the asymptotic expansions for $\omega_{2,3\pm}$, $\omega_{4,5\pm}$ and $\omega_{6,7\pm}$ given

by Eqs. (20)–(22). It is not surprising at all because $\omega_{2,3\pm}$, $\omega_{4,5\pm}$ and $\omega_{6,7\pm}$ are the values of ω for which Eq. (6) has double roots with respect to k .

Now we substitute $\omega = \bar{\omega}_{dj} + a\lambda + ia\sigma$ ($j = 1, \dots, 6$) in Eq. (6) considered as an equation for k , and look for the solutions in the form of power series with respect to a . Since Eq. (6) is a fifth-order algebraic equation with respect to k , there are five roots for any value of ω . However we are only interested in roots that may have a nonzero imaginary part.

We start from $j = 1$ and take $\omega = \bar{\omega}_{d1} + a\bar{\omega}$, where $\bar{\omega} = \lambda + i\sigma$. In the zero-order approximation the double root of Eq. (6) is equal to 1, so that we are looking for a solution to Eq. (6) in the form $k = 1 + a\bar{k}$. Substituting these expressions for ω and k in Eq. (6) we arrive at Eq. (25). The solution to this quadratic equation is straightforward and, as a result, we eventually obtain

$$k_1^\pm = 1 + \frac{a}{1 - U^2} \left[U\bar{\omega} - \frac{a(U + 1)}{4(1 - b^2)} \pm iD^{1/2} \right] + \mathcal{O}(\chi^{1/2}a^3), \tag{39}$$

where

$$\begin{aligned} D &= \frac{a^3\bar{\omega}(1 - U)}{8(1 - b^2)^2} - \left[\bar{\omega} - \frac{a(1 + U)}{4(1 - b^2)} \right]^2 \\ &\quad - \frac{a^2\bar{\omega}(1 + b^2)}{(1 - b^2)^2} \left[\bar{\omega} - \frac{a(1 + U)}{4(1 - b^2)} \right]. \end{aligned} \tag{40}$$

Recall that $\chi = 1$ when $\bar{\omega} \sim 1$ and $\chi = a^2$ when $|\bar{\omega}| \leq a$. We are only interested in k -roots that have nonzero imaginary part when $\sigma = 0$. It is easy to see that, when $\bar{\omega}$ is real and the expression in the first square brackets on the right-hand side of Eq. (40) is larger or of the order of a , $D < 0$ and $\Im(k_1^\pm) = 0$. Hence we can have $\Im(k_1^\pm) \neq 0$ at $\sigma = 0$ only if

$$\Re(\bar{\omega}) \equiv \lambda = \frac{a(1 + U)}{4(1 - b^2)} + a^2\xi, \tag{41}$$

where ξ is an arbitrary parameter. Then it immediately follows that $D > 0$ if and only if

$$\xi^2 < \frac{1 - U^2}{32(1 - b^2)^3}. \tag{42}$$

This inequality can be satisfied only if $|U| < 1$. Since we consider either $U < -1$ or $U > b$, we impose the restriction $b < U < 1$. When σ is of the order of unity, we obtain

$$k_1^\pm = 1 - \frac{ia\sigma}{U \mp 1} + \mathcal{O}(a^2), \tag{43}$$

which implies that $\Im(k_1^+) > 0$ and $\Im(k_1^-) < 0$ when $\sigma = \gamma_M/a + \epsilon$. Since $\Im(k_1^+) > 0$ and $\Im(k_1^-) < 0$ at $\sigma = 0$, we conclude that the trajectory of $k_1^+(\sigma)$ starts and ends in the upper part of the complex plane, and the trajectory of $k_1^-(\sigma)$ starts and ends in the lower part of the complex plane. This result implies that the roots k_1^\pm do not give rise to spatially amplifying waves when $|x| \rightarrow \infty$.

Let us now proceed to $j = 2$. We note that if a pair (ω, k) satisfies Eq. (6), then the pair $(-\omega^*, -k^*)$ also satisfies Eq. (6). This means that Eq. (6) has the roots $k_2^\pm = -(k_1^\pm)^*$ when

$\omega = -\bar{\omega}_{d2} - a\lambda + ia\sigma$. Hence, in this case the trajectories of the two complex roots are symmetric with respect to the imaginary axis to the trajectories of the roots in the case $j=1$. Therefore, they also do not give rise to spatially amplifying waves as $|x| \rightarrow \infty$.

Now we take $j=3$. In this case Eq. (6) has a double root $k=2/(1+b)$ in the zero-order approximation. Substituting $\omega = \bar{\omega}_{d3} + a\bar{\omega}$ and $k=2/(1+b) + a\bar{k}$ in Eq. (6), we obtain Eq. (28). The solutions of this equation are

$$\begin{aligned} \bar{k}_3^\pm &= \frac{(b-1-2U)\bar{\omega}}{2(U+1)(U-b)} \\ &\pm \frac{i[(1-b)(U+1)(U-b) - b(1+b)^4\bar{\omega}^2]^{1/2}}{2b^{1/2}(1+b)(U+1)(U-b)} \\ &+ \mathcal{O}(a^2). \end{aligned} \tag{44}$$

We see that $\Im(\bar{k}_3^\pm) \neq 0$ at $\sigma=0$ only if

$$\lambda^2 < \frac{(1-b)(U+1)(U-b)}{b(1+b)^4}. \tag{45}$$

Long but straightforward calculation results in

$$\begin{aligned} 2(2b)^{1/2}(1+b)(U+1)(U-b)\Im(\bar{k}_3^\pm) &= (2b)^{1/2}(1+b)(b \\ &- 1 - 2U)\sigma \pm \{[(b(1+b)^4(\lambda^2 + \sigma^2) - (1-b)(U+1) \\ &\times (U-b))^2 + 4b(1-b)(1+b)^4(U+1)(U-b)\sigma^2]^{1/2} \\ &- b(1+b)^4(\lambda^2 - \sigma^2) + (1-b)(U+1)(U-b)\}^{1/2}. \end{aligned} \tag{46}$$

Let us first consider $U < -1$. Then $b-1-2U > 0$ and we immediately obtain that $\Im(k_3^+) > 0$ for any $\sigma \geq 0$. Hence, the whole trajectory of $k_3^+(\sigma)$ is in the upper part of the complex plane and k_3^+ does not give rise to spatially amplifying waves as $|x| \rightarrow \infty$.

The condition $\Im(\bar{k}_3^-) > 0$ can be reduced to

$$\sigma^2 > \left(\frac{\gamma_M}{a}\right)^2 - \frac{(1+b)^2\lambda^2}{(b-1-2U)^2}. \tag{47}$$

Hence, $\Im(k_3^-) > 0$ at $\sigma = \gamma_M/a + \epsilon$ so that the trajectory of $k_3^-(\sigma)$ starts in the upper and ends in the lower part of the complex plane. Since $\Im(k_3^-) < 0$ at $\sigma=0$, this implies that the root k_3^- gives rise to a spatially amplifying wave as $x \rightarrow \infty$ if λ satisfies Eq. (45).

Now we consider $U > b$. In this case $b-1-2U < 0$ and we immediately see that $\Im(k_3^-) < 0$ for any $\sigma \geq 0$. Hence, the whole trajectory of $k_3^-(\sigma)$ is in the lower part of the complex plane and k_3^- does not give rise to spatially amplifying waves as $|x| \rightarrow \infty$. The condition that $\Im(\bar{k}_3^+) < 0$ is once again reduced to Eq. (47). Hence, $\Im(k_3^+) < 0$ at $\sigma = \gamma_M/a + \epsilon$, so that the trajectory of $k_3^+(\sigma)$ starts in the lower part of the complex plane and ends in the upper part. Since $\Im(k_3^+) > 0$ at $\sigma=0$, this implies that the root k_3^+ gives rise to a spatially amplifying wave as $x \rightarrow -\infty$ if λ satisfies Eq. (45).

In the case when $j=4$ the trajectories of the roots $k_4^\pm(\sigma)$ are symmetric to the trajectories of the roots $k_3^\pm(\sigma)$ with respect to the imaginary axis if we take $\omega = \bar{\omega}_{d4} - a\lambda + ia\sigma$. This

implies that k_4^- gives rise to a spatially amplifying wave as $x \rightarrow \infty$ when $U < -1$, and k_4^+ gives rise to a spatially amplifying wave as $x \rightarrow -\infty$ when $U > b$.

Let us now take $j=5$. In this case Eq. (6) has a double root $k = -2/(1-b)$ in the zero order approximation. Substituting $\omega = \bar{\omega}_{d5} + a\bar{\omega}$ and $k = -2/(1-b) + a\bar{k}$ in Eq. (6), we obtain Eq. (31). The discriminant of this quadratic equation is equal to

$$(1-b)^2\bar{\omega}^2 + \frac{(1+b)(U+1)(U+b)}{b(1-b)^2}. \tag{48}$$

It is positive when $\sigma=0$ and either $U < -1$ or $U > b$. Hence, the roots k_5^\pm do not give rise to spatially amplifying waves as $|x| \rightarrow \infty$. By symmetry, the same is true for $j=6$.

Summarizing, we conclude that there are spatially amplifying waves only if

$$\omega_d = \pm \frac{2(b-U)}{1+b} + a\lambda, \tag{49}$$

where λ satisfies Eq. (45). When $U < -1$, there is a spatially amplifying wave propagating in the positive x -direction. When $U > b$, there is a spatially amplifying wave propagating in the negative x -direction. In both cases the spatial amplification rate is given by

$$|\Im(k_3^\pm(0))| = \frac{a[(1-b)(U+1)(U-b) - b(1+b)^4\lambda^2]^{1/2}}{2b^{1/2}(1+b)(U+1)(U-b)}. \tag{50}$$

The wavenumber of a spatially amplifying wave is $k = \pm 2/(1+b) + \mathcal{O}(a)$.

V. SUMMARY AND CONCLUSIONS

In this paper we have studied the absolute and convective instabilities of circularly polarized Alfvén waves (pump waves) propagating along the ambient magnetic field. We have restricted our analysis to the decay instability which occurs when $b < 1$ (recall that b is the ratio of the sound and Alfvén speeds). To make analytical progress we have assumed that the amplitude of the pump wave a is small and used expansions in power series with respect to a . We have shown that the circularly polarized Alfvén wave is absolutely unstable in a reference frame moving with the velocity Uv_A with respect to the rest plasma in the direction of Alfvén wave propagation if U satisfies $U_l < U < U_r$, where $U_l = -1 + \mathcal{O}(a)$ and $U_r = b + \mathcal{O}(a^2)$. The instability increment takes its maximum value given by Eq. (10) when $U = (b-1)/2$.

When either $U < -U_l$ or $U > U_r$, the circularly polarized Alfvén wave is convectively unstable. In this case we have studied the signaling problem. We have found that the signaling with the frequency $\omega_d\omega_0$, where ω_0 is the frequency of the pump wave, gives rise to spatially amplifying waves only if $\omega_d = \pm 2(b-U)/(1+b) + a\lambda$, where λ satisfies the inequality Eq. (45). These spatially amplifying waves propagate in the positive x -direction when $U < -1$, and in the negative x -direction when $U > b$, where the positive x -direction is the direction of propagation of the pump wave with respect to

the rest plasma. The wavenumber of a spatially amplifying wave is $\pm 2k_0/(1+b) + \mathcal{O}(a)$, where k_0 is the wavenumber of the pump wave.

The results obtained in this paper can have serious implication on the interpretation of observational data obtained in space missions. Alfvén waves propagating in the solar wind plasma have been observed during space missions. Since the Alfvén speed is much smaller than the solar wind speed at distances of the order of or larger than 1 a.u. (astronomical unit), the phase speed of Alfvén waves in the solar reference frame is approximately equal to the solar wind speed. The speeds of space stations with respect to the solar reference frame are much smaller than the solar wind speed. This means that the phase speed of Alfvén waves is approximately equal to the solar wind speed in a space station reference frame, i.e., it is much larger than the Alfvén speed. In accordance with the results obtained in this paper this implies that circularly polarized Alfvén waves propagating in the solar wind plasma are always convectively unstable in a space station reference frame. Hence, we cannot observe temporal growth of the Alfvén wave instability in space missions.

What we can observe during space missions are the spatially amplifying waves produced by this instability. However, to make such observations is not simple at all. The reason is that the characteristic scale of spatial amplification is very large. If we take as typical values $v_A = 50$ km/s and $v_{\text{sol}} = 500$ km/s, where v_{sol} is the solar wind speed, then we obtain for the dimensionless velocity of a space station relative to the solar wind $|U| \approx 10$. It follows from Eq. (50) that, for b not very close to zero, which is usually the case in the solar wind, $|\mathcal{I}(k_3^\pm(0))| \lesssim a/|U| \approx a/10$. Then the spatial amplification scale is $L \gtrsim k_0^{-1} |\mathcal{I}(k_3^\pm(0))|^{-1} \approx 10k_0^{-1} a^{-1}$. Let us consider an Alfvén wave with period T_0 . The period of this wave in the solar wind reference frame is approximately $T_0 v_{\text{sol}}/v_A$ and its frequency is $\omega_0 = 2\pi v_A (T_0 v_{\text{sol}})^{-1} \approx 0.6/T_0$. Then, using the relation $\omega_0 = v_A k_0$, we eventually arrive at $L \gtrsim 17v_A T_0/a$. The typical value for T_0 is 1 hour. Taking $a = 0.1$ we obtain $L \gtrsim 2.5 \times 10^7$ km = 1/6 a.u. In view of this result it is not surprising at all that evidence of the decay instability of Alfvén waves in the solar wind is sparse.²⁶

ACKNOWLEDGMENTS

M.S.R. acknowledges the support of the U.K.'s PPARC (Particle Physics and Astronomy Research Council). D.S. ac-

knowledges the support by the University of Sheffield Endowment Fellowship.

- ¹A. A. Galeev and V. N. Oraevskii, *Sov. Phys. Dokl.* **7**, 988 (1963).
- ²R. Z. Sagdeev and A. A. Galeev, *Non-linear Plasma Theory* (Benjamin, New York, 1969).
- ³N. F. J. Derby, *Astrophys. J.* **224**, 1013 (1978).
- ⁴M. L. Goldstein, *Astrophys. J.* **219**, 700 (1978).
- ⁵J. Mio, T. Ogino, K. Minami, and S. Takeda, *J. Phys. Soc. Jpn.* **41**, 265 (1976).
- ⁶J. Mio, T. Ogino, K. Minami, and S. Takeda, *J. Phys. Soc. Jpn.* **41**, 667 (1976).
- ⁷E. Mjølhus, *J. Plasma Phys.* **16**, 321 (1976).
- ⁸C. R. Ovenden, H. A. Shah, and S. J. Schwartz, *J. Geophys. Res.* **88**, 6095 (1983).
- ⁹S. R. Spangler and J. P. Sheerin, *J. Plasma Phys.* **27**, 193 (1982).
- ¹⁰S. R. Spangler and J. P. Sheerin, *Astrophys. J.* **272**, 273 (1983).
- ¹¹J. I. Sakai and B. U. Ö Sonnerup, *J. Geophys. Res.* **88**, 9069 (1983).
- ¹²M. Longtin and B. U. Ö Sonnerup, *J. Geophys. Res.* **91**, 6816 (1986).
- ¹³H. K. Wong and M. L. Goldstein, *J. Geophys. Res.* **91**, 5617 (1986).
- ¹⁴G. Brodin and L. Stenflo, *Phys. Scr.* **37**, 89 (1988).
- ¹⁵A. F. Viñas and M. L. Goldstein, *J. Plasma Phys.* **46**, 129 (1991).
- ¹⁶S. Ghosh, A. F. Viñas, and M. L. Goldstein, *J. Geophys. Res.* **98**, 15561 (1993).
- ¹⁷S. Ghosh, A. F. Viñas, and M. L. Goldstein, *J. Geophys. Res.* **99**, 19289 (1994).
- ¹⁸S. Ghosh and M. L. Goldstein, *J. Geophys. Res.* **99**, 13351 (1994).
- ¹⁹J. V. Hollweg, R. Esser, and V. Jayanti, *J. Geophys. Res.* **98**, 3491 (1993).
- ²⁰V. Jayanti and J. V. Hollweg, *J. Geophys. Res.* **99**, 23449 (1994).
- ²¹K. M. Ling and B. Abraham-Shrauner, *J. Geophys. Res.* **84**, 6713 (1979).
- ²²S. R. Spangler, *Phys. Fluids B* **1**, 1738 (1989).
- ²³S. R. Spangler, *Phys. Fluids B* **2**, 407 (1990).
- ²⁴B. Inhester, *J. Geophys. Res.* **95**, 10525 (1990).
- ²⁵Y.-Q. Low, *Mon. Not. R. Astron. Soc.* **279**, L67 (1996).
- ²⁶S. R. Spangler, in *Nonlinear Waves and Chaos in Space Plasmas*, edited by T. Hada and H. Matsumoto (Terrapub, Tokyo, 1997), p. 171.
- ²⁷L. Del Zanna, M. Velli, and P. Londrillo, *Astron. Astrophys.* **367**, 705 (2001).
- ²⁸L. Del Zanna, M. Velli, and P. Londrillo, in *Solar Wind Ten*, edited by M. Velli, R. Bruno, and F. Malara (American Institute of Physics, 2003), p. 566.
- ²⁹L. Del Zanna and M. Velli, *Adv. Space Res.* **30**, 471 (2002).
- ³⁰V. Jayanti and J. V. Hollweg, *J. Geophys. Res.* **98**, 13247 (1993).
- ³¹M. S. Ruderman and D. Simpson, *J. Plasma Phys.* **70**, 143 (2004).
- ³²R. J. Briggs, *Electron-stream interaction with plasmas* (MIT press, Cambridge, MA, 1964).
- ³³A. Bers, in *Survey Lectures. Proc. Int. Congr. Waves and Instabilities in Plasmas*, edited by G. Auer and F. Cap (Institute for Theoretical Physics, Innsbruck, Austria, 1973), p. B1.
- ³⁴P. Huerr and P. A. Monkewitz, *J. Fluid Mech.* **159**, 151 (1985).
- ³⁵L. Brevdo, *Geophys. Astrophys. Fluid Dyn.* **40**, 1 (1988).
- ³⁶A. N. Wright, K. J. Mills, M. S. Ruderman, and L. Brevdo, *J. Geophys. Res.* **105**, 385 (2000).
- ³⁷M. T. Terra-Homem and R. Erdélyi, *Astron. Astrophys.* **403**, 425 (2003).
- ³⁸M. T. Terra-Homem and R. Erdélyi, *Astron. Astrophys.* **413**, 7 (2004).
- ³⁹V. Jayanti and J. V. Hollweg, *J. Geophys. Res.* **98**, 19049 (1993).